Journal of Thermal Analysis, Vol. 12 (1977) 245–263

SIMULTANEOUS DTA–EGA OF MINERALS AND NATURAL MINERAL MIXTURES

D. J. MORGAN

Institute of Geological Sciences, 64/78 Gray's Inn Road, London WC1X 8NG, U. K.

(Received February 18, 1977)

A DTA apparatus has been linked to non-dispersive infrared H_2O and CO_2 analyzers and an SO_2 analyzer based on an electrochemical cell, enabling evolution profiles of these three volatiles to be recorded simultaneously with the DTA curve. Examples are given of the use of the combined DTA–EGA method in the determination of the quantitative mineralogical composition of potential industrial raw materials.

The present report describes results from simultaneous DTA–EGA of minerals and mineral mixtures obtained by linking a Stanton Redcroft 673–4 DTA apparatus to commercially available H_2O and CO_2 non-dispersive infrared detectors* and an SO_2 detector** based on an electrochemical cell. Emphasis is placed on the quantitative aspects of the combined method, examples being taken mainly from material examined during a continuing work programme of the Mineralogy Unit, Institute of Geological Sciences, aimed at the assessment of non-metallic minerals as potential industrial raw materials.

The measurement of volatiles evolved from minerals on heating, when carried out simultaneously with DTA, may not only provide additional insight into the decomposition behaviour of individual minerals but also yield quantitative data for certain constituents of natural mineral mixtures. Many methods for measuring volatiles have been described [1, 2] but for minerals one is concerned primarily with the measurement of cooled water, carbon dioxide and sulphur dioxide. A variety of methods have been used for the detection and measurement of these three volatiles. Creer et al. [3] measured H_2O evolution from clay minerals and hydrated aluminas and iron oxides with an electrolytic hygrometer, some runs being carried out simultaneously with TG. Lomas [4] used moist air to transport SO_2 evolved on heating pyrite to an absorption bottle containing hydrogen peroxide, the conductivity of which was measured continuously by means of an electrical bridge circuit. A conductivity method was also employed by Keattch [5]

* Manufactured by the Analytical Development Co. Ltd., Pindar Road, Hoddesdon, Hertfordshire, UK.

** 'Air Pollution Monitor' manufactured by Environmental Products Division of Whittaker Corp., 9100 Independence Avenue, Chatsworth, California, U.S.A.

to measure CO_2 evolved during the thermal decomposition of calcareous materials. The 'thermo-gas-titrimetric' method used by Kenyeres et al. [6] to measure SO_2 and CO_2 released during simultaneous DTA–TG–DTG of impure bauxites is based on a similar principle except that the pH of the absorbing solution is monitored. Measurement of the heat of adsorption of H_2O on calcium hydride was employed by Kulbicki and Grim [7] to study dehydration and dehydroxylation reactions in a number of mineral groups. Similarly, heats of adsorption of SO_2 and CO_2 on lead peroxide and 'ascarite', respectively, were used by Chantret [8] to monitor evolution of these volatiles during DTA of sediments containing sulphides, carbonates and organic matter. Volatiles released during DTA of an impure clay containing pyrite, organic matter and siderite have been monitored by quadrupole mass spectrometry [9]. This simultaneous method shows by far the greatest flexibility with regard to the number of volatiles which can be detected but, in spite of advances in design of valve sampling devices necessary to overcome the different operating conditions of DTA equipment and a mass spectrometer, cannot yet be regarded as fully quantitative.

Experimental

Description of equipment

A photograph of the complete DTA–EGA system is shown in Fig. 1. Volatiles released during the DTA run are transported through the restricted top exit of the furnace, along a stainless steel cooling line, to the three detectors arranged in series. Concentrations in the carrier gas of up to 10,000 ppm H_2O and CO_2, and up to 1,000 ppm SO_2, can be measured. Output signals from the detectors are fed into a multichannel chart recorder (Rikadenki model KA-41) which also monitors T and ΔT.

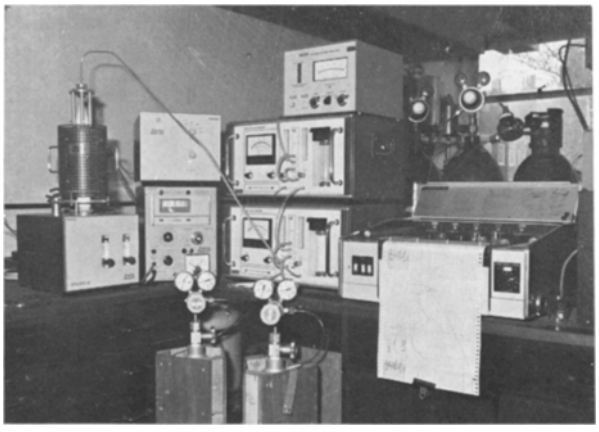

Fig. 1. The DTA–EGA system. The H_2O analyzer (bottom) is first in series followed by the CO_2 and SO_2 analyzers. Two cylinders containing calibration gases are in the foreground

The carrier gas normally consists of a 2:1 mixture by volume of nitrogen and oxygen and enters the bottom of the furnace at a total flow rate of 300 ml/min. Proportions of the two components of the carrier gas mixture can be varied by means of flowmeters located at the front of the furnace base module; accurate measurement of carrier gas flow rate is made by flowmeters at the inlet port of each analyzer. A gas-tight seal between furnace tube and base module is maintained by means of a silicone rubber 'O' ring.

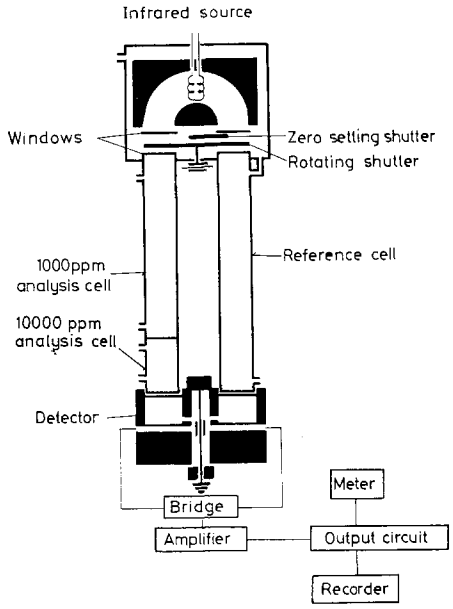

Fig. 2. Schematic diagram of infrared H_2O and CO_2 analyzers

A slight modification of the furnace assembly was necessary to accommodate the stainless steel cooling line. This passes through the centre of a machined duralumin support which fits on to three duralumin pillars bolted to a sindanyo ring forming the top of the furnace housing. The tube (o.d. 4.0 mm, i.d. 2.0 mm) was originally 'ground-in' to the furnace exit (i.d. 3.5 mm) using fine carborundum paste, a gas-tight fit being maintained subsequently by a compression spring between the duralumin support and a collar on the tube. The cooling line, which is 0.5 m long, is connected to the first detector by a short length of polypropylene tubing, this material also being used for all connections within and between detectors.

Both H_2O and CO_2 detectors (Fig. 2) utilize the fact that each infrared absorbing gas possesses a unique absorption spectrum. Two beams of infrared radiation of equal energy are interrupted by a rotating shutter which allows the beams to pass intermittently but simultaneously through an analysis cell assembly and a parallel

reference cell and thence into a detector. This is filled with a sample of the type of gas to be measured and is divided symmetrically into two chambers by a pressure-sensitive diaphragm. The reference cell is filled with a non-absorbing (monatomic) gas. When the sample gas is passed through the analysis cell it absorbs energy to which the detector is sensitized and the resulting energy imbalance between the two chambers causes deflection of the diaphragm. Insulated electrodes forming capacitors on either side of the diaphragm are connected to an electronic bridge circuit to detect diaphragm movement. The resulting analogue signal is amplified

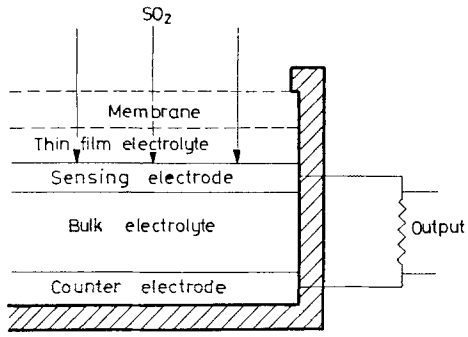

Fig. 3. Schematic diagram of SO_2 analysis cell (the selectivity of the cell to SO_2 is achieved by the unique membrane/electrolyte/electrode combination, the composition of which is not released by the manufacturers of the detector)

and displayed on a meter calibrated over the range of measurement. The analysis cell assembly contains two cells, one capable of measuring concentrations in the range 0–1,000 ppm H_2O or CO_2, the other concentrations in the range 0–10,000 ppm. Connection to the appropriate cell is made via a mimic diagram on the front panel of the detector. Calibration is by means of standard gases containing 900 ppm H_2O or CO_2 in nitrogen.

The SO_2 detector (Fig. 3) is based on a fuel cell. Sulphur dioxide in the carrier gas diffuses through a semi-permeable membrane and is adsorbed on a sensing electrode where it undergoes electro-oxidation. The resulting current, which is directly proportional to the partial pressure of SO_2 in the carrier gas, is amplified and the output displayed on a meter. The detector has three switch settings for measurement of 0–100, 0–300 and 0–1,000 ppm SO_2. Calibration is by a standard gas containing 800 ppm SO_2 in nitrogen.

Quantitative measurements

Concentrations of the three volatiles in the carrier gas stream are measured continuously by the separate detectors and presented graphically against temperature or time as evolution profiles. Since the flow rate of the carrier gas is constant, the total volume of each volatile can be calculated by integration of its evolution

profile. The total weight of volatile can then be found by utilizing the fact that the molecular weight of any gas occupies 22.414 ml at STP. It should be emphasized that, regardless of the temperature at which the volatile is evolved, the cooling effect of the stainless steel line is sufficient to ensure that the gas stream enters the detectors at ambient air temperature. Measurement of volatiles in the carrier gas is made at 28°, the stable running temperature of the detectors.

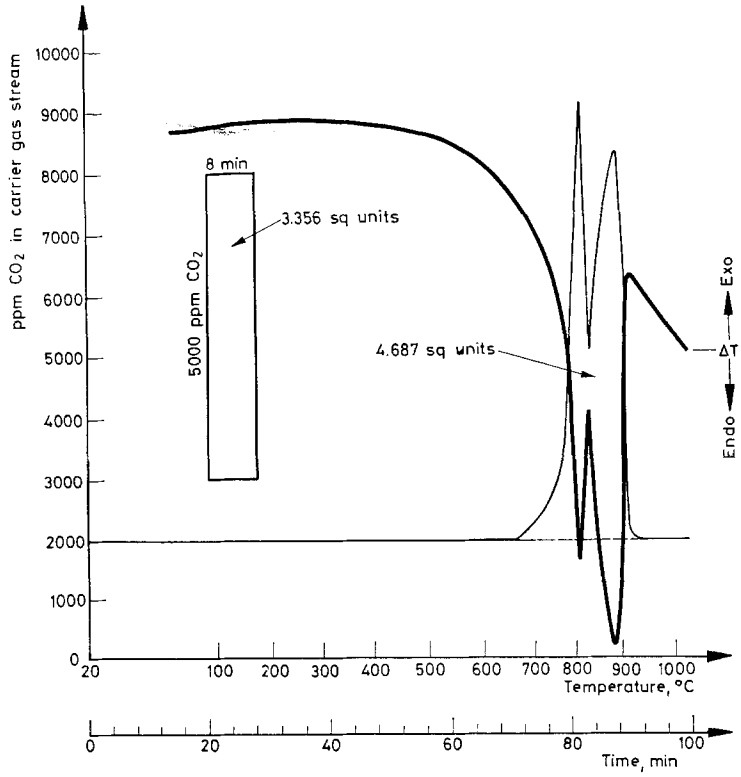

Fig. 4. DTA—EGA of dolomite. Sample weight: 65.6 mg; reference material: αAl_2O_3; heating rate: 10°/min; carrier gas: 2 : 1 mixture of N_2 and O_2 at 300 ml/min. Note: For clarity of presentation the CO_2-evolution profile baseline has been moved to 2000 ppm

The method of calculation may be illustrated by reference to Fig. 4, which shows the DTA curve and corresponding CO_2-evolution profile of a sample of dolomite (U.S. National Bureau of Standards No. 88a). A rectangular area of roughly the same order of magnitude as that of the volatile evolution profile is first defined on the original chart. The calibration area in this instance represents a constant concentration of 5,000 ppm CO_2 in the carrier gas stream for a period of 8 min.

As the flow rate of the carrier gas is 300 ml/min,* the corresponding volume of CO_2 is:

$$\frac{5{,}000}{1{,}000{,}000} \times 300 \times 8 = 12 \text{ ml.}$$

The molecular weight of CO_2 (44.01 g) occupies 22,414 ml at STP or $22{,}414 \times \frac{301}{273}$ ml at 28°.

The weight of CO_2 corresponding to the calibration area is thus

$$44.01 \times 12 \times \frac{273}{22{,}414 \times 301} = 21.4 \text{ mg}$$

Both calibration area and the area of the CO_2-evolution profile are then measured with a planimeter and the weight of CO_2 corresponding to the latter area obtained by comparison. For the present sample this procedure gave a CO_2 content of 29.8 mg, the actual value being 30.6 mg.

It may be inferred from the method outlined above that accurate quantitative determinations depend on a number of factors, by far the most important being the accuracy of the standard gas used for calibrating the detector. This is normally supplied with a possible error of $\pm 5\%$ of the stated concentration but is subjected to a further, independent, analysis prior to use. Once calibrated, the accuracy of the detectors is within $\pm 1\%$ of full scale reading. Measurement of the carrier gas flow rate, the next most important potential source of error, is by flowmeters located at the inlet port of each analyzer. These are calibrated for air and corrections must be made when other gases are used. Potential errors accompanying planimeter measurement of calibration area and area of the volatile evolution profile are minimized as far as possible by taking the mean of several determinations.

Time lag between volatile evolution and detection

The relatively fast carrier gas flow rate used should, in theory, ensure that the delay between recording the reaction responsible for volatile generation (DTA signal) and actual detection of the volatile (EGA signal) is very small in relation to the time scale of a normal DTA – EGA run. For CO_2 and SO_2, visual monitoring of departures from baseline of corresponding DTA and volatile evolution peaks indicates a time lag of the order of 5 seconds for the first detector in series and no more than 10 seconds for the subsequent detector. For H_2O, however, temporary condensation between furnace and analysis cell results in an appreciable delay between evolution and detection. This is illustrated in Fig. 5 by the DTA –

* The small contribution to the total flow rate made by the evolved CO_2 is ignored here for simplicity.

EGA curves of malachite, a copper hydroxycarbonate which decomposes above 300° with simultaneous evolution of H_2O and CO_2. It is apparent that the H_2O-profile 'peaks' later than both DTA endotherm and CO_2 profile (despite the fact that the CO_2 detector followed the H_2O detector in series). The lag is of the order

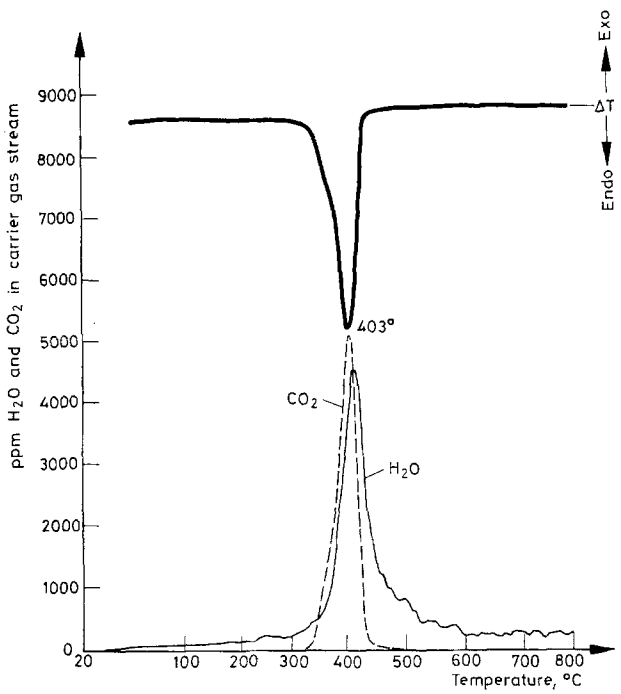

Fig. 5. DTA—EGA of malachite. Sample weight 59.2 mg (diluted 1 : 1 with αAl_2O_3); reference material: αAl_2O_3; heating rate: 10°/min; carrier gas: 2 : 1 mixture of N_2 and O_2 at 300 ml/min

of 30 seconds or 5° at the heating rate employed. Measurement of the area of the H_2O evolution profile gave 8.40% H_2O, which is sufficiently close to the theoretical value of 8.15% to suggest that all the evolved H_2O eventually reached the detector. Close agreement was also obtained between measured (19.33%) and theoretical (19.90%) CO_2 contents.

Quantitative determination of sulphide minerals

An important factor which has to be taken into account when carrying out quantitative determinations on sulphide minerals is the composition of the sample atmosphere, as this influences the path along which decomposition occurs and, consequently, the amount of SO_2 evolved. Quantitative determinations are pos-

sible, provided the correct experimental conditions are chosen. Figs 6a and b show SO_2-evolution profiles for pyrite (FeS_2) and sphalerite (ZnS). Pure oxygen was used as the carrier gas and, in order to minimize self-generated atmosphere effects, the samples were spread thinly over the base of a shallow alumina crucible placed on top of the DTA head. Amounts of SO_2 evolved were as predicted by the equations representing complete oxidation, viz.:

$$4\,FeS_2 + 11\,O_2 \rightarrow 2\,Fe_2O_3 + 8\,SO_2$$
$$2\,ZnS + 3\,O_2 \rightarrow 2\,ZnO + 2\,SO_2$$

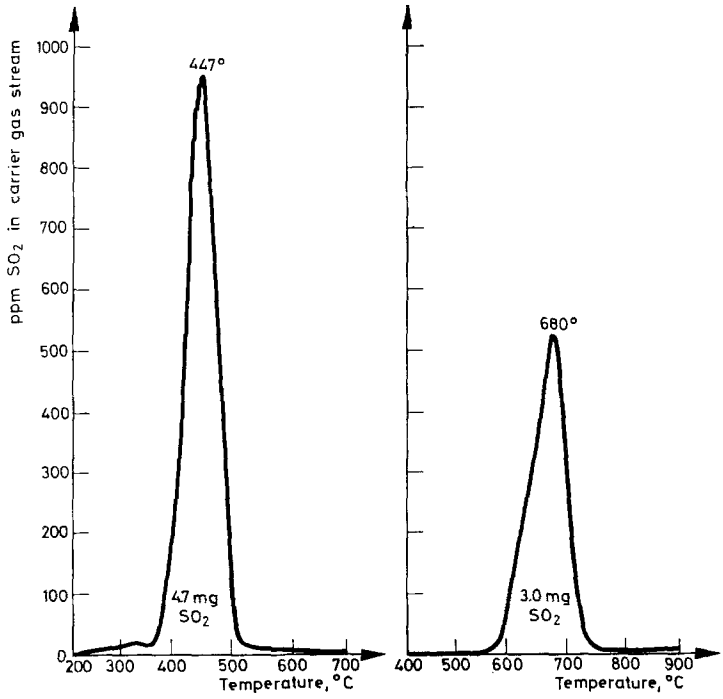

Fig. 6. EGA of pyrite (a) and sphalerite (b). Sample weight: 4.50 mg; sample particle size: 50–63 μm; sample holder: shallow alumina crucible; heating rate: 10°/min; carrier gas: O_2 at 300 ml/min

The SO_2-evolution profile for pyrite shows a number of pulses immediately preceding the main peak. Similar pulses were noted by Bollin [10] during high resolution DTA of pyrite under oxidative conditions using a flat pan sample holder, and were ascribed to variations in surface energies of sites at which oxidation is initiated either in individual particles or particle groups.

Circumstances completely different to those described above prevail during DTA–EGA of sulphide-bearing mineral mixtures. The sample is packed in a crucible and has limited access to the furnace atmosphere. As a result, the sample

atmosphere rapidly becomes saturated with reaction gases and intermediate products of the sulphide decomposition, notably sulphates, may form. These sulphates decompose at higher temperatures liberating SO_3. Above 400°, SO_3 is unstable and undergoes partial dissociation to SO_2 and O_2. The degree of dissociation increases with increase in temperature although dissociation is not complete until about 1200° [11]. However, if the extent of dissociation of SO_3 to SO_2 within a particular temperature interval is known, it is possible to estimate the total SO_3 evolved and hence the amount of intermediate sulphate product. Two examples of sulphates which liberate SO_3 at different temperatures are given below.

DTA–EGA of alunite and $CuSO_4 \cdot 5H_2O$

Figure 7 shows the DTA–EGA curves of alunite, $KAl_3(SO_4)_2(OH)_6$, which loses structural H_2O between 500 and 600° and $^3/_4$ of its SO_3 content between 800 and 900° [12, 13]. The weight of SO_2 calculated from the area of the evolution profile indicates 40% dissociation of the SO_3 liberated in this temperature interval. Figure 8 shows the DTA–EGA curves of $CuSO_4 \cdot 5\,H_2O$. Decomposition of the anhydrous sulphate takes place via the oxysulphate $CuO \cdot CuSO_4$, and both DTA curve and SO_2-evolution profile reflect the two-stage nature of the decomposi-

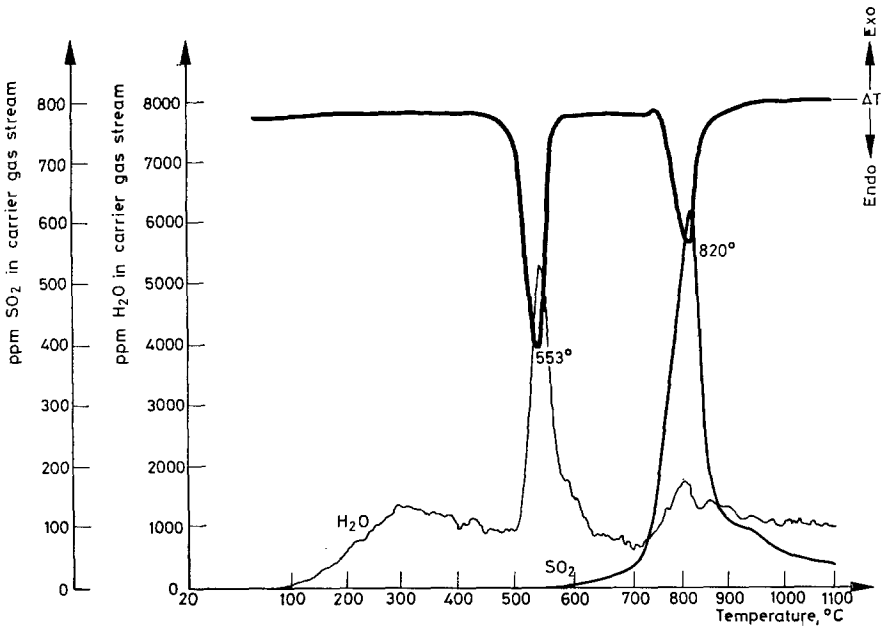

Fig. 7. DTA–EGA of alunite. Sample weight: 36.9 mg (diluted 1 : 4 with αAl_2O_3); reference material: αAl_2O_3; heating rate: 10°/min; carrier gas: 2:1 mixture of N_2 and O_2 at 300 ml/min

tion. The weight of SO_2 corresponding to the total area of the evolution profile indicates that, at this higher temperature, 60% of the liberated SO_3 dissociates to SO_2.

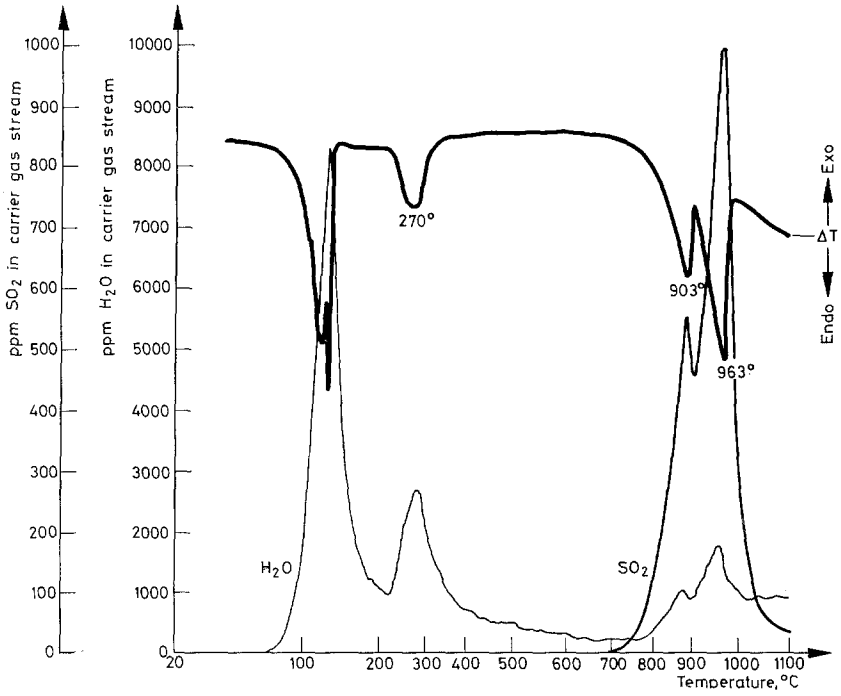

Fig. 8. DTA—EGA of $CuSO_4 \cdot 5\ H_2O$. Sample weight: 39.3 mg (diluted 1 : 4 with αAl_2O_3); reference material: αAl_2O_3; heating rate: 10°/min; carrier gas: 2 : 1 mixture of N_2 and O_2 at 300 ml/min

Estimation of pyrite in shale

The above data on the dissociation of SO_3 was put to use in the estimation of the amount of pyrite in a black, carbonaceous Cambrian shale, one of a number which gave rise to electromagnetic anomalies during an air-borne survey of the Harlech Dome, North Wales. DTA—EGA curves are shown in Fig. 9. The SO_2-evolution profile shows two peaks between 350 and 450°, both of which relate to the production of SO_2 according to the oxidation reaction given above. Simultaneous disproportionation of part of the FeS_2 to FeS also occurs, most of this lower valency sulphide oxidizing immediately to $FeSO_4$ and $Fe_2(SO_4)_3$ [14]. The peak at 525° on the SO_2-profile represents combustion of a small amount of unreacted FeS [15]. The intermediate products $FeSO_4$ and $Fe_2(SO_4)_3$ decompose at 700 and

900°, respectively, producing SO_3 which partially dissociates to SO_2 and O_2 as described previously. Measurement of the areas of all the peaks on the SO_2 evolution profile gave a total of 6.66% SO_2. Assuming values of 30% and 60% respectively for the dissociation of SO_3 liberated from $FeSO_4$ and $Fe_2(SO_4)_3$ would

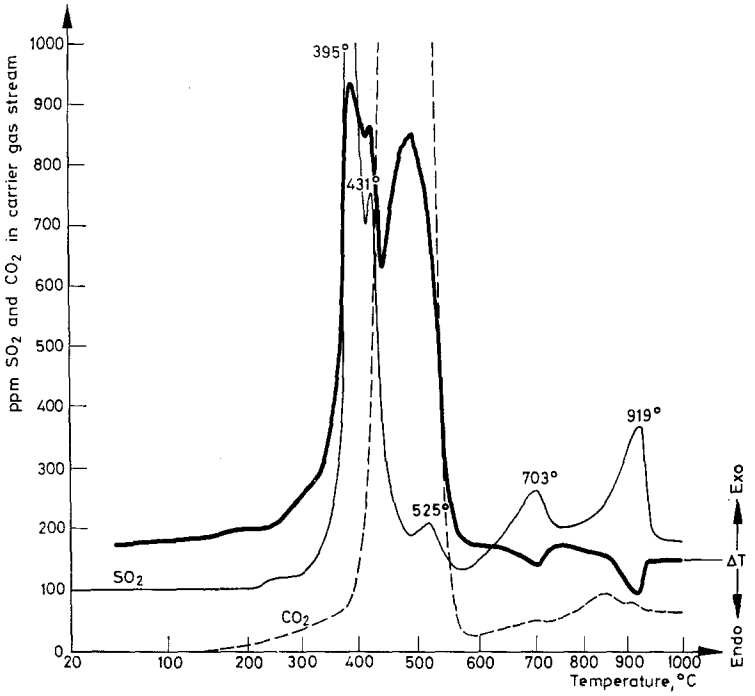

Fig. 9. DTA—EGA of pyritiferous shale, Harlech Dome, North Wales. Sample weight: 184.3 mg; reference material: αAl_2O_3; heating rate: 10°/min; carrier gas: 2 : 1 mixture of N_2 and O_2 at 300 ml/min. Note: SO_2-evolution profile baseline raised to 100 ppm

suggest a further 0.74% SO_2 equivalent to the undissociated SO_3. The final figure of 7.40% SO_2 is equivalent to 6.9% pyrite. Subsequent chemical analysis of the shale (analyst: Mrs. S. A. Rizzello) gave 7.51% SO_2 which is equivalent to 7.0% pyrite.

Applications in applied mineralogy

Determination of graphite in schist

DTA—EGA carried out under different flowing gas compositions provided a simple yet elegant means of determining the amount of graphite in a graphite-calcite-schist from Kanbe, Burma, this information being required prior to attempts to upgrade the material.

The DTA curve (Fig. 10), obtained under a 2 : 1 nitrogen oxygen mixture, shows a large exothermic effect due to graphite combustion and, superimposed on this, an endothermic peak resulting from dissociation of the calcite. The area of the corresponding CO_2-evolution profile, represented as a solid line in the figure, gives the amount of CO_2 generated during both reactions. By heating the

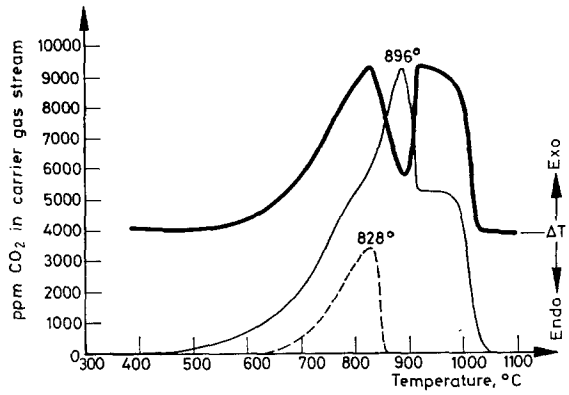

Fig. 10. DTA—EGA of graphite-calcite-schist, Kanbe, Burma. Sample weight: 98.2 mg; reference material: αAl_2O_3; heating rate: 10°/min; carrier gas flow rate: 300 ml/min. DTA curve and CO_2-evolution profile represented as solid line obtained with 2 : 1 mixture of N_2 and O_2, CO_2-profile represented as dashed line obtained with pure N_2 carrier gas

sample in pure nitrogen, combustion of graphite was completely suppressed and only CO_2 from the calcite dissociation was recorded. The CO_2-profile obtained under nitrogen is represented as a dashed line in the figure (it may be noted that calcite dissociated much earlier in the absence of the CO_2 atmosphere generated in the sample by graphite combustion). Subtraction of the area of this peak (equivalent to 46.6% calcite) from the area of the larger peak gave the amount of CO_2 generated by graphite combustion and, from this, the amount of graphite (26.5%) was calculated.

Determination of impurities in fuller's earths

Fuller's earth, which consists essentially of the clay mineral Ca-montmorillonite, has a number of commercial uses [16], one of the more important being the bleaching or decolourizing of glyceride and mineral oils. The decolourizing action is greatly enhanced by acid treatment which removes Al and other cations from the octahedral layer of the montmorillonite, thereby altering the pore-size distribution and modifying the surface chemistry of the clay. By varying the amount of acid attack, a series of grades of bleaching clay are produced, efficient use of the acid depending on a knowledge of the amount and type of impurities, especially carbonates, in the natural fuller's earth.

Figure 11 shows the DTA – EGA curves of a fuller's earth from one of the four deposits currently being worked in the UK. The large initial endotherm on the DTA curve corresponds to the loss of adsorbed and cation-bound water from the montmorillonite. Dehydroxylation of the clay (a two-stage process) occurs be-

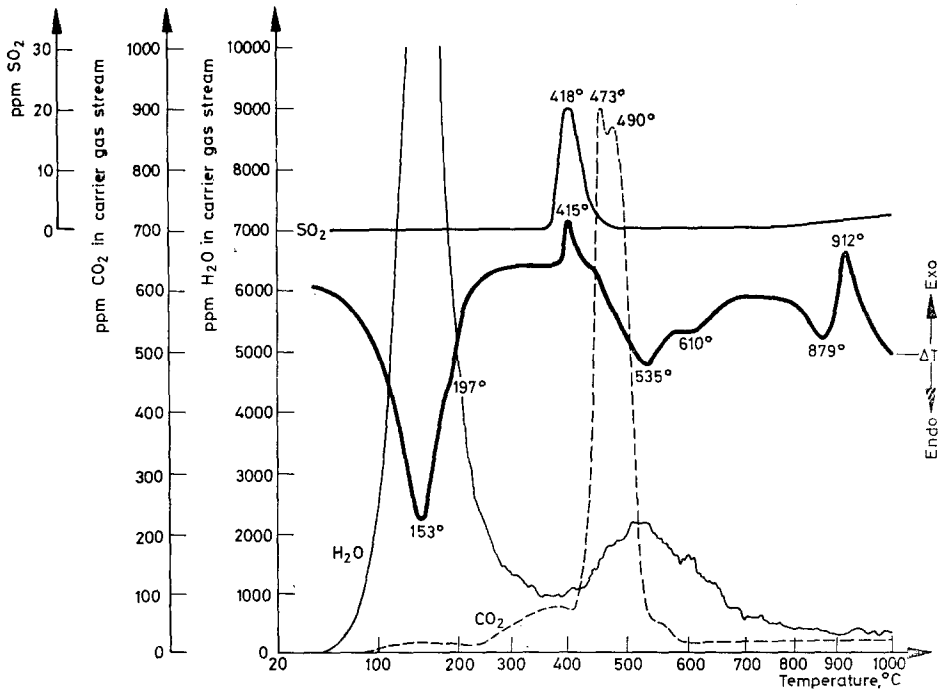

Fig. 11. DTA—EGA of fuller's earth, Lower Greensand, Nutfield, Surrey. Sample weight: 184.0 mg; reference material: αAl_2O_3; heating rate: 10°/min; carrier gas: 2 : 1 mixture of N_2 and O_2 at 300 ml/min

tween 450 and 700°, recrystallization of the resulting amorphous product taking place between 800 and 950°. The exotherm at 415° represents oxidation of 0.2% pyrite impurity (amount calculated from the area of the corresponding peak on the SO_2-evolution profile). Combustion of 0.1% organic matter is responsible for the broad shallow CO_2 peak between 100 and 600°. The large CO_2 peak results from dissociation of 4.1% siderite ($FeCO_3$) impurity. No indication of the presence of this mineral was obtained from the DTA curve. This is due to the cancelling out of the endothermic effects accompanying CO_2 loss by the simultaneous exothermic oxidation of the FeO dissociation product to Fe_2O_3.

Determination of the composition of talc-rich rocks

Deposits of talc, $Mg_3Si_4O_{10}(OH)_2$, occur in a metamorphic environment associated either with ultrabasic rocks or dolomitic limestones. Impurities are mainly Mg-rich carbonates (magnesite and dolomite) or silicates (chlorite, tremolite and minerals of the serpentine group). All of these, together with talc, lose volatiles in stoichiometric amounts at temperatures below 1100°, and are thus amenable to

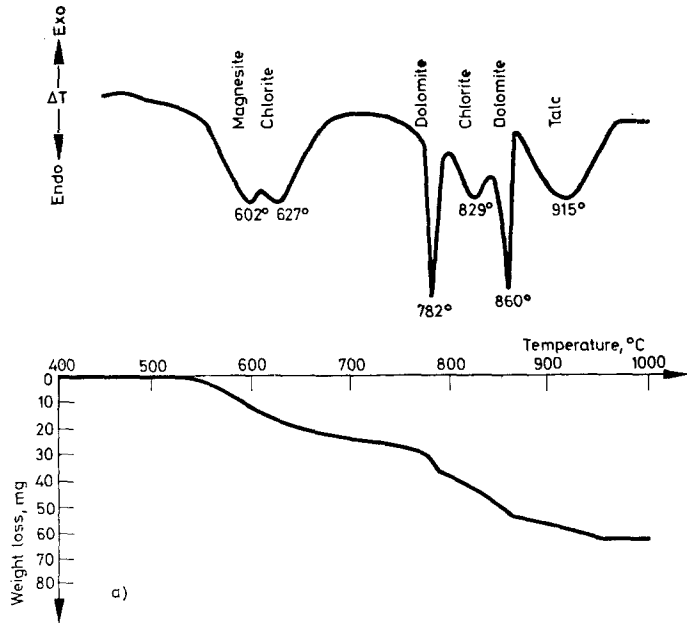

Fig. 12a. TG–DTA of altered ultrabasic rock, Cornwall. Sample weight: 491.1 mg; reference material: αAl_2O_3; heating rate: 6°/min; atmosphere: static air

measurement by thermoanalytical techniques. Simultaneous TG–DTA has been used successfully in the assessment of talc-magnesite rocks from Shetland [17], weight losses from these two minerals being separated by a sufficiently large temperature interval. However, in multi-component mixtures of talc and impurities, weight losses from separate constituents may often overlap and quantitative interpretation is difficult.

Figure 12a shows the simultaneous TG–DTA curves of an altered ultrabasic rock from Cornwall. Apart from talc, major amounts of magnesite, dolomite and chlorite are present. Interpretation of the weight loss curve is further complicated by the fact that two of the constituents, dolomite and chlorite, dissociate in two stages. Only talc can be determined with any degree of confidence, the weight loss above 870° giving a value of 41 % for this mineral. Accurate magnesite

and dolomite contents can, however, be calculated from the areas of the CO_2 peaks obtained by simultaneous DTA–EGA of the sample (Fig. 12b). Values of 5.0% magnesite and 12.4% dolomite were obtained. Values for chlorite and talc were not so easily obtained from the corresponding H_2O-evolution profile due to difficulty in resolving the final H_2O loss of chlorite from the talc H_2O loss.

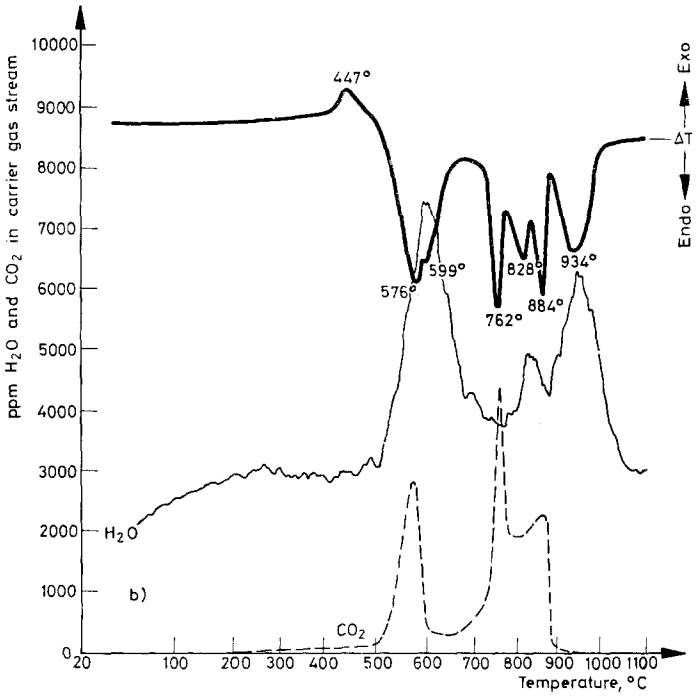

Fig. 12b, DTA–EGA of altered ultrabasic rock, Cornwall. Sample weight: 232.2 mg; reference material: αAl_2O_3; heating rate: 15°/min; carrier gas: 2 : 1 mixture of N_2 and O_2 at 300 ml/min. Note: H_2O-evolution profile baseline raised to 2000 ppm

However, if the H_2O value equivalent to the 41% talc obtained from TG–DTA is subtracted from the total amount of H_2O equivalent to the area of the evolution profile from 500 to 1050°, then the H_2O remaining gives a figure of 34% for the chlorite content. Magnetite is the only other mineral present in significant amount, this being responsible for the exotherm at 447° on the DTA curve in Fig. 12b.

Appraisal of ceramic raw materials

The suitability of the so-called 'common' clays for the manufacture of building bricks, hollow tiles, drain pipes and other constructional ceramics is assessed primarily on the basis of such criteria as plasticity, drying shrinkage, rigidity in

the dried state, the presence of fluxing constituents capable of causing incipient vitrification at moderate kiln temperatures, and the strength of the fired body [18]. Certain constituents of the raw clay, e.g. carbonates, sulphides and organic matter, may be undesirable in large amounts. Carbonate minerals, for instance, adversely affect plasticity, evolve large volumes of gas near the vitrification temperature (which may increase porosity of the fired body) and, being active fluxes, cause short firing ranges. Scumming and efflorescences may also appear on weathering of a ceramic body originally containing pyrite and carbonate, due to interaction of these minerals on firing to produce water-soluble sulphates. Pyrite and organic matter, especially when they occur together, may cause bloating and black-coring, unless a long oxidation is provided during firing. The identification and measurement of such constituents may therefore be important in the assessment programme and here DTA – EGA has an obvious and useful role to play. A less obvious application of the combined technique is described below.

The bloating behaviour of certain types of clays and shales is actually utilized in the production of expanded aggregate for lightweight concrete [19]. Bloating is achieved by introducing the clay, usually as lumps or pellets, into a furnace maintained at a temperature of about 1200°. Fusion of the clay takes place

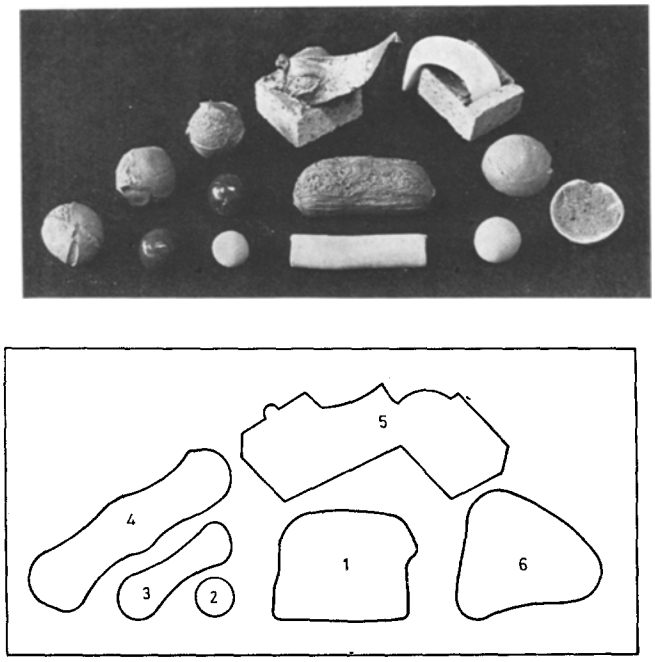

Fig. 13. Products from bloating trials on Lower Palaeozoic clay, Scotland. 1: extruded test bar and bloated product, 2: green test pellet, 3: product from slow firing of 2, 4: bloated product of 2 (note disrupted skin), 5: sample test cone and Seger Cone no 6A (1215°), 6: commercial bloating clay; green test pellet and products (note vesicular texture and smooth outer skin)

simultaneously with volatile generation from various accessory constituents and, provided sufficient glass of the appropriate viscosity is produced, the volatiles remain trapped in the melt. Cooling produces lightweight aggregate of high mechanical strength, each lump, although porous inside, having a thin oxidized vitreous skin.

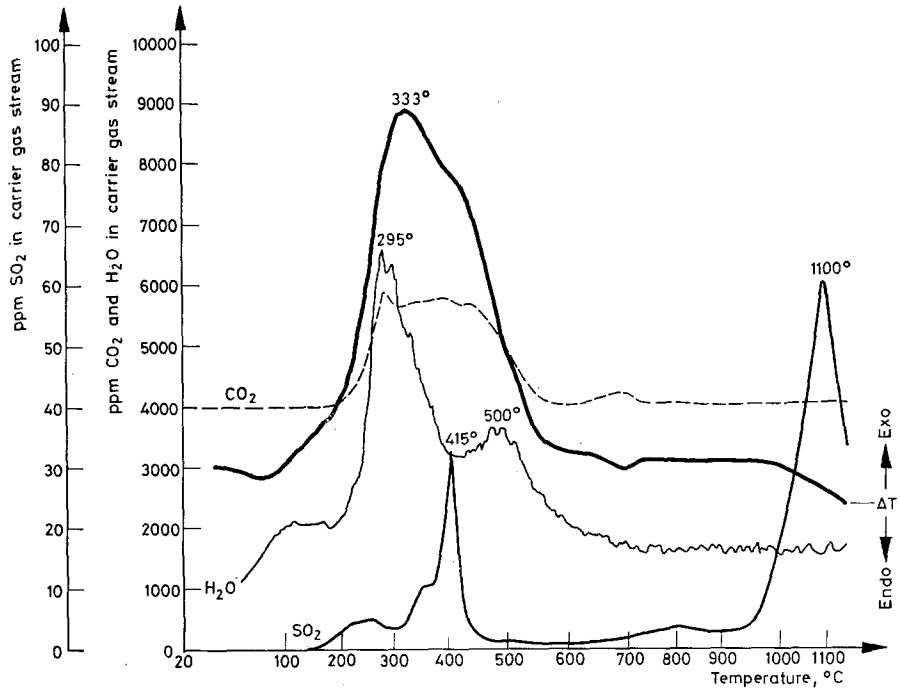

Fig. 14. DTA–EGA of Lower Palaeozoic clay, Scotland. Sample weight: 213.4 mg; reference material: αAl_2O_3; heating rate: 10°/min; carrier gas: 2 : 1 mixture of N_2 and O_2 at 300 ml/min. Note: H_2O- and CO_2-evolution baselines raised to 1000 and 4000 ppm, respectively

Figure 13 shows some of the products obtained from laboratory trials on the bloating behaviour of a Lower Palaeozoic shale from Scotland. Small trial pellets did show marked bloating, and high mechanical strength aggregate was produced. It was very difficult, however, to contain the porous body within an unruptured skin, the fired pellets giving the impression of having blown out at the surface too vigorously. In an attempt to explain this behaviour, a DTA–EGA run was carried out on the original clay (Fig. 14). From this it is apparent that there are two generations of volatile evolution. Between 100 and 600°, CO_2 is produced from combustion of organic matter and SO_2 from combustion of pyrite (about 6% organic matter and 0.1% pyrite are present). The H_2O peak at 295° results from the breakdown of organic matter and that at 500° from dehydroxylation of

clay minerals. Apart from a small amount of CO_2 resulting from the decomposition of 0.5% calcite at about 700°, no further volatile generation takes place until 1000° when SO_2 is again recorded. This results from dissociation of SO_3 evolved during the decomposition of $CaSO_4$ (originally present as gypsum). The amount of organic carbon in the sample is about three times that recorded by White [19] as the optimum value for self-bloating clays and shales. An excess of bloating gases is thus the most likely reason for the observed rupturing of the vitreous skin of the heated product. However, it is possible that some rupturing resulted from later evolution of SO_3/SO_2 from gypsum, especially if, as is likely, this mineral occurs at an appreciably larger grain size than the other constituents of the clay.

*

Acknowledgement is due to Mr. G. R. Brumby who constructed the stainless steel cooling line. This paper is published by permission of the Director, Institute of Geological Sciences.

References

1. W. LODDING, Gas Effluent Analysis, Arnold, London, 1967.
2. A. VERDIN, Gas Analysis Instrumentation, Macmillan, London, 1973.
3. M. H. CREER, J. C. B. HARDY, H. P. ROOKSBY and J. E. STILL, Clay Miner., 9 (1971) 19.
4. H. LOMAS, Trans. Brit. Ceram. Soc., 65 (1966) 337.
5. C. J. KEATTCH, Analysis of Calcareous Materials, S.C.I. Monogr. no. 18, 1964, p. 279.
6. S. KENYERES, P. GADÓ, M. SAJÓ and K. SOLYMÁR, Proc. 4th Intern. Congr. Thermal Anal. (Budapest), Akadémiai Kiadó, Vol. 2, 1975, p. 531.
7. G. KULBICKI and R. E. GRIM, Mineralog Mag., 32 (1959) 53.
8. F. CHANTRET, Bull. Soc. Franc. Mineral. Crist., 92 (1969) 462.
9. M. MULLER-VONMOOS and R. MULLER, Proc. 4th Intern. Congr. Thermal Anal. (Budapest), Akadémiai Kiadó, Vol. 2, 1975, p. 521.
10. E. M. BOLLIN, Differential Thermal Analysis 1 (ed. R. C. Mackenzie), Academic Press, New York 1970.
11. G. NICKLESS, Inorganic Sulphur Chemisty, Elsevier, 1968.
12. G. M. GADD, J. Am. Ceram. Soc., 33 (1950) 208.
13. M. A. KASHKAI and I. A. BABAEV, Mineralog Mag., 37 (1969) 128.
14. F. PAULIK, S. GÁL and L. ERDEY, Anal. Chim. Acta, 29 (1963) 381.
15. T. KENNEDY and B. T. STURMAN, J. Thermal Anal., 8 (1975) 329.
16. D. E. HIGHLEY, Fuller's Earth, Mineral Resources Consultative Committee, Mineral Dossier No. 3, HMSO London, 1972.
17. J. A. BAIN, D. A. BRIGGS and F. MAY, Trans. Inst. Min. Metall. (Sect. B: Appl. earth sci.) 80 (1971) 77.
18. J. A. BAIN, Proc. 1st Industrial Minerals Congr. (Metal Bulletin Ltd., London), 1975, p. 240.
19. W. A. WHITE, Circular 290, Illinois State Geological Survey, Urbana, 1960.

RÉSUMÉ — On a couplé un appareil d'analyse thermique différentielle avec un spectromètre infrarouge non dispersif pour l'analyse d'H_2O et CO_2 et avec une cellule électrochimique pour l'analyse de SO_2, afin d'enregistrer simultanément la courbe ATD et le profil de dégagement de ces trois composés volatils. On donne des exemples d'application de ce couplage dans la détermination de la composition minéralogique quantitative de matières premières potentielles de l'industrie.

ZUSAMMENFASSUNG — Ein DTA-Gerät wurde mit nicht-dispersiven Infrarot-Analysatoren für H_2O und CO_2 sowie mit einem auf einer elektrochemischen Zelle beruhenden SO_2-Analysator gekoppelt, welche die gleichzeitige Registrierung der Entwicklungsprofile dieser drei flüchtigen Substanzen und der DTA-Kurve gestatten. Beispiele zum Einsatz der kombinierten DTA—EGA-Methode bei der Bestimmung der quantitativen mineralogischen Zusammensetzung potentieller Rohstoffe der Industrie werden gegeben.

Резюме — ДТА прибор был соединен с не диспергирующими инфракрасными анализаторами H_2O и CO_2, а также с каким-либо SO_2 анализатором на основе электрохимической ячейки, что давало возможность снимать профильное выделение этих трех летучих веществ одновременно с кривой ДТА. Даны примеры использования комбинированного ДТА-ЕГА метода при определении количественного минералогического состава потенциально-промышленных сырьевых материалов.